

An Improved ATP FRET Sensor For Yeast Shows Heterogeneity During Nutrient Transitions

Dennis Botman, Johan H. van Heerden, and Bas Teusink*

Cite This: *ACS Sens.* 2020, 5, 814–822

Read Online

ACCESS |

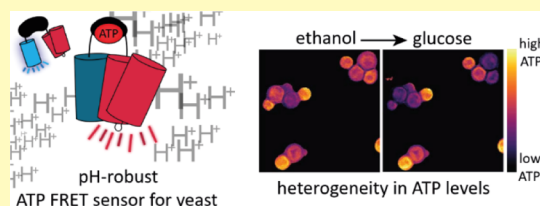
Metrics & More

Article Recommendations

Supporting Information

ABSTRACT: Adenosine 5-triphosphate (ATP) is the main free energy carrier in metabolism. In budding yeast, shifts to glucose-rich conditions cause dynamic changes in ATP levels, but it is unclear how heterogeneous these dynamics are at a single-cell level. Furthermore, pH also changes and affects readout of fluorescence-based biosensors for single-cell measurements. To measure ATP changes reliably in single yeast cells, we developed yAT1.03, an adapted version of the AT1.03 ATP biosensor, that is pH-insensitive. We show that pregrowth conditions largely affect ATP dynamics during transitions. Moreover, single-cell analyses showed a large variety in ATP responses, which implies large differences of glycolytic startup between individual cells. We found three clusters of dynamic responses, and we show that a small subpopulation of wild-type cells reached an imbalanced state during glycolytic startup, characterized by low ATP levels. These results confirm the need for new tools to study dynamic responses of individual cells in dynamic environments.

KEYWORDS: ATP, single-cell, heterogeneity, budding yeast, biosensor, FRET



Adenosine 5-triphosphate (ATP) is one of the key players in cellular metabolism as it is the major Gibbs energy-carrier for most if not all species.^{1,2} ATP is produced either by proton-gradient driven ATPases or by substrate-level phosphorylation. The latter occurs in glycolysis, the central metabolic pathway in many organisms, including human. A key question is how pathway flux is regulated under dynamic conditions, which not only happens in nature and biotechnical processes,^{3–6} but also in humans.^{7–9} Given the task of glycolysis to produce ATP, it is not a surprise that the glycolytic flux is (also) regulated by ATP itself.^{10,11}

Saccharomyces cerevisiae (or budding yeast) has been the focus of many studies of glycolysis; when it encounters an environmental change to glucose-rich conditions, glycolysis rapidly becomes active.^{12–14} For glycolysis to run, an initial investment of two ATPs in the upper part (the conversion from glucose to fructose-1,6-bisphosphate) is needed, which is succeeded by a return of four ATPs in the lower part (the conversion from glyceraldehyde-3-phosphate to pyruvate, in twofold, Figure 1). When glucose is added, the initial and rapid use of ATP thus creates an (temporarily) imbalance between the two parts of glycolysis, resulting in a transient decrease of ATP levels.^{14–16} The initial difference in flux between the two parts of glycolysis can recover, resulting in a balanced state. However, the upper glycolysis flux can also continue to exceed the lower glycolysis flux, resulting in an imbalanced state.^{16–18}

These studies therefore suggested that startup of glycolysis can be highly variable, with a small fraction of cells dynamically ending up in an imbalanced metabolic state.¹⁷ This can be important for industrial processes in which metabolic subpopulations can affect industrial efficiency.^{3–6} Such varia-

bility could also have implications for therapeutic efficiencies in human diseases.^{19–22} These conclusions, however, were based on computational modeling and indirect evidence; in particular, pH was used as an indirect readout of metabolism not ATP itself. There is a need, therefore, to directly monitor ATP dynamics at the single cell level and establish a low ATP, imbalanced state. However, continuous measurements of ATP, and hence glycolytic startup dynamics have not been studied at a single-cell level.

In recent years, several fluorescence-based biosensors for in vivo monitoring of ATP in single cells have been developed, including the AT1.03 and the QUEEN sensor.^{23,24} However, these sensors use fluorescent proteins (FPs) that are pH-sensitive in the physiological range, where the intracellular pH of budding yeast operates.^{17,25–29} In fact, the pH transiently drops exactly during glycolytic startup.^{17,30} Moreover, the metabolic imbalanced state leads to an inability to maintain pH homeostasis, resulting in a significant drop in intracellular pH, making the sensors unsuitable to study ATP dynamics during glycolytic startup. Therefore, we adapted the AT1.03 sensor to become less pH-sensitive. This modified sensor, denoted yAT1.03, is pH-robust and can be used to reliably detect single-cell ATP dynamics.

Received: December 14, 2019

Accepted: February 20, 2020

Published: February 20, 2020

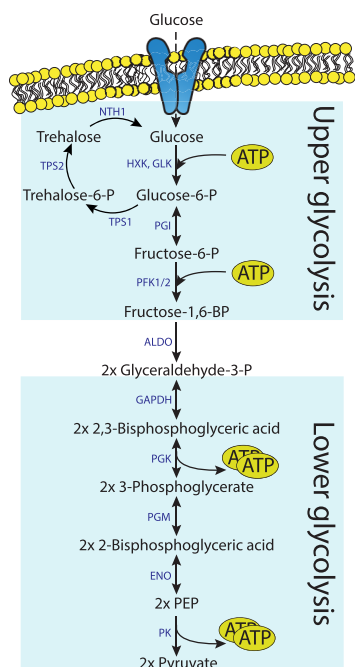


Figure 1. Schematic overview of glycolysis. Startup of glycolysis requires an investment of two ATP molecules in the upper part of glycolysis. Lower part of glycolysis yields four ATP afterward.

MATERIALS AND METHODS

yAT1.03 Construction. The ATP sensor AT1.03 and its inactive variant AT1.03^{R122KR126K} in the yeast expression vector pDRF1-GW were a gift from Wolf Frommer (Addgene plasmids #28003 and #28005, respectively). First, an EcoRI restriction site was removed by performing a PCR on AT1.03 and AT1.03^{R122KR126K} pDRF-GW using KOD polymerase (Merck-Millipore, Burlington, Massachusetts, USA) with the forward primer 5'-ATACTAGTGCTAGCTCTAGACTC-GAGTATGGTGAG-3' and reverse primer 5'-ATAGCGGCCGCT-GATCAGCGGTTTAAACTTAAAGC-3'. Next, the product and pDRF1-GW were digested using SpeI and NotI (New England Biolabs, Ipswich, Massachusetts, USA), and the PCR product was ligated into pDRF1-GW using T4 ligase (New England Biolabs). Next, a PCR was performed on tdTomato pDRF1-GW using FW primer 5'-ATGAATT-CATGGTGAGCAAGGGC-3' and RV primer 5'-ATGCGGCCGCT-TACTTGTACAGCTCGTCCA-3'. The PCR product and the new AT1.03 and AT1.03^{R122KR126K} in pDRF1-GW were digested with EcoRI (New England Biolabs) and NotI. Afterward, the PCR product was ligated into AT1.03 and AT1.03^{R122KR126K} in pDRF1-GW using T4 ligase, which replaced cp173-mVenus with tdTomato. Next, a PCR using KOD polymerase was performed on ymTq2 pDRF1-GW with FW primer 5'-CTGCTAGCACTAGTAAGCTTTTAA-3' and RV primer 5'-ATATCGATAGCAGCAGTAACGAATTCC-3', which produced ymTq2 with the last 11 amino acids removed (ymTq2Δ11). The PCR product and AT1.03 and AT1.03^{R122KR126K} in pDRF1-GW were digested with NheI and ClaI (New England Biolabs). Next, the PCR product was ligated into AT1.03 and AT1.03^{R122KR126K} in pDRF1-GW using T4 ligase, which produced AT1.03^{ymTq2Δ11-tdTomato} and AT1.03^{R122KR126K-ymTq2Δ11-tdTomato}, named yAT1.03 and yAT1.03^{R122KR126K}.

Yeast Transformation. The yeast strain W303-1A (MATa, leu2-3/112, ura3-1, trp1-1, his3-11/15, ade2-1, can1-100) was transformed as described by Gietz and Schiestl.³¹

ConA Solution. Concanavalin A was prepared, as described by Hansen et al., 2015.³² Briefly, 5 mg of concanavalin A (type IV, Sigma-Aldrich) was dissolved in 5 mL of phosphate-buffered saline at pH 6.5, 40 mL of H₂O, 2.5 mL of 1 M MnCl₂, and 2.5 mL of 1 M CaCl₂. This solution was aliquoted, snap-frozen, and stored at −80 °C.

In Vitro Characterization. W303-1A WT cells expressing yAT1.03 pDRF-GW and the empty pDRF1-GW vector were grown overnight at 200 rpm and 30 °C in 1× yeast nitrogen base without amino acids (YNB, Sigma-Aldrich, St. Louis, MO, USA), containing 100 mM glucose (Boom BV, Meppel, Netherlands), 20 mg/L adenine hemisulfate (Sigma-Aldrich), 20 mg/L L-tryptophan (Sigma-Aldrich), 20 mg/L L-histidine (Sigma-Aldrich), and 60 mg/L L-leucine (SERVA Electrophoresis GmbH, Heidelberg, Germany). Next, cells were diluted in 50 mL of medium and grown to an OD₆₀₀ of approximately 3. Cells were kept on ice and washed twice with 20 mL of 0.01 M KH₂PO₄/K₂HPO₄ buffer at pH 7 containing 0.75 g/L ethylenediaminetetraacetic acid (EDTA) (AppliChem GmbH, Darmstadt, Germany). Next, cells were resuspended in 2 mL of 0.01 M KH₂PO₄/K₂HPO₄ buffer containing 0.75 g/L EDTA and washed twice in 1 mL of ice-cold 0.1 M KH₂PO₄/K₂HPO₄ buffer at pH 7.4 containing 0.4 g/L MgCl₂ (Sigma-Aldrich). Cells were transferred to screw cap tubes containing 0.75 g of glass beads (425–600 μm) and lysed using a FastPrep-24 5G (MP Biomedicals, Santa Ana, CA, USA) with 8 bursts of 6 m/s and 10 s. Last, the lysates were centrifuged for 15 min at 21,000g, and the cell-free extracts were snap-frozen in liquid nitrogen.

Per sample, 5 wells of a black 96-well microtiter plate (Greiner Bio-One) were filled with 4 μL of cell-free extract (10× diluted in distilled water) and 36 μL of 10 mM HEPES–KOH buffer (Sigma-Aldrich) at various pHs. Fluorescence spectra were recorded after subsequent additions of ATP (Sigma-Aldrich) using a CLARIOstar plate reader (BMG labtech, Ortenberg, Germany). Spectra were obtained using 430/20 nm excitation and 460–660 nm emission (10 nm bandwidth). Fluorescence spectra were corrected for background fluorescence (by correcting for fluorescence of cell-free extract of cells expressing the empty pDRF1-GW plasmid), and Förster resonance energy transfer (FRET) ratios were calculated by dividing acceptor over donor fluorescence. Changes of ATP levels in the cell-free extracts were measured by measuring the FRET levels in time at either 0.3 or 1.1 mM ATP. The dose–response curve was fitted to eq 1,²³ with FRET_{max} and FRET_{min} denoting the maximal and minimal FRET values obtained, respectively, ATP the ATP concentration (mM), *k_d* the dissociation constant (mM), and *n* the Hill coefficient (*n*).

$$\text{FRET} = \frac{(\text{FRET}_{\text{max}} - \text{FRET}_{\text{min}}) \times \text{ATP}^n}{\text{ATP}^n + k_d^n} + \text{FRET}_{\text{min}} \quad (1)$$

Microscopy. Cells expressing yAT1.03 or yAT1.03^{R122KR126K} were grown overnight at 200 rpm and 30 °C in 1× YNB medium, containing 20 mg/L adenine hemisulfate, 20 mg/L L-tryptophan, 20 mg/L L-histidine, 60 mg/L L-leucine, and either 1% ethanol (v/v, VWR International, Radnor, PA, United States of America), 100 mM fructose (Sigma-Aldrich), or 111 mM galactose (Sigma-Aldrich). Next, cells were diluted in the same medium and grown overnight to a maximum OD₆₀₀ of 1.5 (midlog). Afterward, the cells were transferred to a six-well plate containing ConA-coated coverslips. Coverslips with the attached cells were put in an Attotfluor cell chamber (Thermo Fisher Scientific, Waltham, MA, USA), and 1 mL of fresh medium was added. Next, the coverslips were imaged using a Nikon Ti-eclipse widefield fluorescence microscope (Nikon, Minato, Tokyo, Japan) at 30 °C equipped with a TuCam system (Andor, Belfast, Northern Ireland) containing 2 Andor Zyla 5.5 sCMOS Cameras (Andor) and a SOLA 6-LCR-SB power source (Lumencor, Beaverton, OR, USA). FRET was recorded using a 438/24 nm excitation filter, a 483/32 nm donor emission filter, and a 593/40 nm acceptor emission filter with a 552 nm long-pass (LP) dichroic filter (all filters from Semrock, Lake Forest, IL, USA). For sensor expression levels, tdTomato was measured using a 570/20 nm filter and a 593/40 nm filter with a 600 LP dichroic mirror. After recording the baseline, 111 μL of 1× YNB containing the necessary amino acids and a 10× amount of the desired substrate was added. For the multiple glucose pulses, subsequent additions of 20, 20, 40, and 80 μL of 50 mM glucose at 3, 10, 17, and 24 min were added to the cell chamber. At least two biological replicates were obtained for each experiment. Cells were segmented by an in-house macro using Fiji (NIH, Bethesda, MD, USA), and moving or dead cells were manually removed.

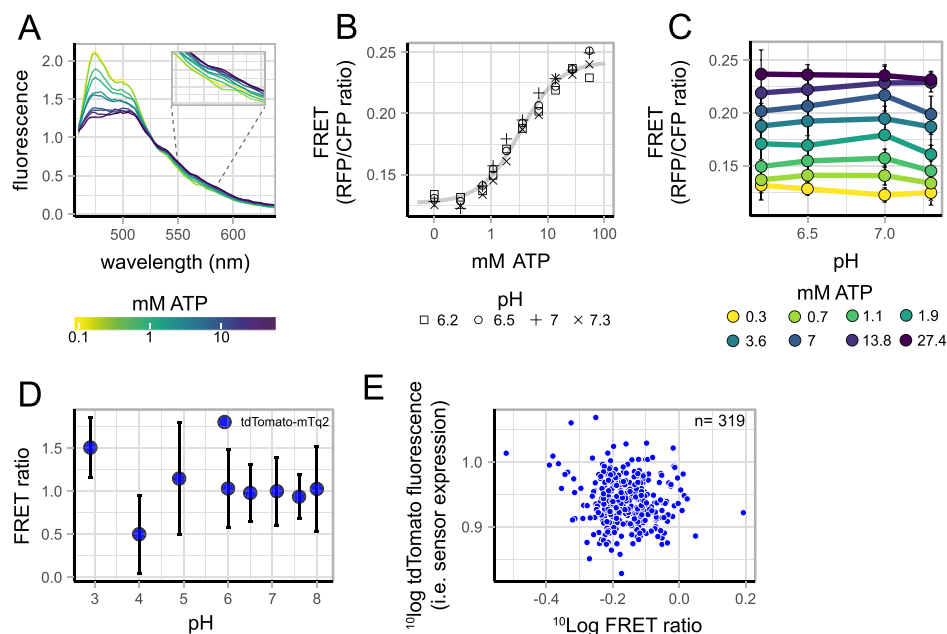


Figure 2. In vitro characterization of yAT1.03. (A) Fluorescence spectra of yAT1.03, obtained from cell-free extracts, gradient color indicates ATP concentration. Inset shows fluorescence values in the acceptor range. (B) Dose–response curve of yAT1.03 obtained from the spectra at various pHs. Points indicate the mean FRET ratio of five replicates, and point shapes indicate pH. (C) pH stability of the sensor at various ATP concentrations, points indicate the mean FRET ratio of five replicates, colors indicate the ATP concentration, and error bars indicate standard deviation. (D) pH stability of the tdTomato-mTq2 FRET pair, measured in vivo through incubation of cells in citric-acid/ Na_2HPO_4 buffers at pH 3–8 with 2 mM DNP. Points indicate the mean FRET ratio and error bars indicate standard deviation. (E) Expression of the sensor, measured as direct acceptor excitation (i.e., tdTomato fluorescence) displayed against the FRET ratio and each point depicts a single cell.

pH Sensitivity of the FRET Pair In Vivo. W303-1A yeast cells expressing the tdTomato-mTq2 were grown, as described for microscopy. Cells were washed twice with sterile water and resuspended in a citrate phosphate buffer [0.1 M citric acid (Sigma-Aldrich) and 0.2 M Na_2HPO_4 (Sigma-Aldrich)] with pH values from 3 to 8 and 2 mM of the ionophore 2,4-dinitrophenol (DNP, Sigma-Aldrich). Cells were loaded on a glass slide. Next, cells were visualized and FRET ratios were determined, as described for microscopy.

Growth Experiments. W303-1a cells expressing yAT1.03 and the empty pDRF1-GW vector or WT cells were grown to midlog, as described for microscopy, with the medium containing 1% ethanol. Cells were washed and resuspended to an OD_{600} of 1 with the same medium without any carbon source. Next, 20 μL of cells was transferred to a 48-well plate with each well containing 480 μL of fresh medium with either 0.1% ethanol, 10 mM galactose, 10 mM fructose, or 10 mM glucose. Afterward, cells were grown in a Clariostar plate reader at 30 °C and 700 rpm orbital shaking. OD_{600} was measured every 5 min.

Data Analysis. R version 3.5.1 (R Foundation for Statistical Computing, Vienna, Austria) was used to analyze and visualize the obtained data. In brief, tdTomato fluorescence was corrected for mTq2 bleedthrough (0.12% of mTq2 fluorescence), and cells with a fluorescence below 500 counts (arbitrary units) were deleted. FRET ratio normalization was performed by dividing all FRET values by the mean FRET value of the baseline (before perturbations). Maximal FRET decrease and increase were determined with a sliding window of three frames. Clustering was performed using the R code made available on Github by Joachim Goedhart (<https://github.com/JoachimGoedhart>). Cluster amounts were determined by using the `fviz_nbclust` function from the `factoextra` package.

RESULTS

yAT1.03 Has Improved pH Robustness. Experiments performed with AT1.03 showed aberrant drifts in the FRET signal in unperturbed cells using our setup (Figure S1). Furthermore, the original paper that reported AT1.03 already showed the pH sensitivity in the range of physiological pH of

yeast.²³ We hypothesized that the baseline drift and the pH sensitivity are caused by the FPs because the donor mseCFP is poorly characterized and mVenus is known to be pH-sensitive and not photostable.²⁵ Based on this, we undertook improvement of AT1.03 by changing the FPs to ymTq2 Δ 11 (donor) and tdTomato (acceptor) as a more reliable and pH-insensitive FRET pair (Botman et al., in submission³³). Replacements of mseCFP for ymTq2 Δ 11 and cp173-mVenus for tdTomato resulted in yAT1.03. In vitro characterization showed a huge improvement in pH sensitivity compared to the original AT1.03 sensor.²³ With the new FPs, FRET ratios, at a fixed ATP concentration (Figure S2), remained stable across the normal physiological pH range (pH 6.25–7.25) of yeast (Figure 2C), indicating that the pH sensitivity of the original AT1.03 sensor indeed arose from the FPs. Because pH sensitivity can be different in vivo compared to in vitro, we checked whether the new FRET pair was also pH-robust in vivo. The new FRET pair showed to be robust to pH values from 8 to 5 in vivo (Figure 2D). Also, no intermolecular FRET was observed as expression levels of yAT1.03 did not affect FRET ratios (Figure 2E). The yAT1.03 sensor showed a k_d of 3.2 mM for ATP, which is almost identical to the original AT1.03. Last, expression of yAT1.03 in W303-1A had no effect on growth (Figure S3), indicating that the sensor can be used without adverse effects on yeast physiology.

yAT1.03 Measures ATP Reliably. In vitro characterization of the sensor showed robust ATP responses of the sensor. To verify that yAT1.03 visualizes ATP changes reliably in vivo as well, we performed several control experiments (Figure 3). First, we tested whether the sensor showed a typical transient change in ATP when cells experience a sudden glucose perturbation (Figure 3A). As expected, yAT1.03 FRET ratios transiently decreased, followed by a recovery, while no response was

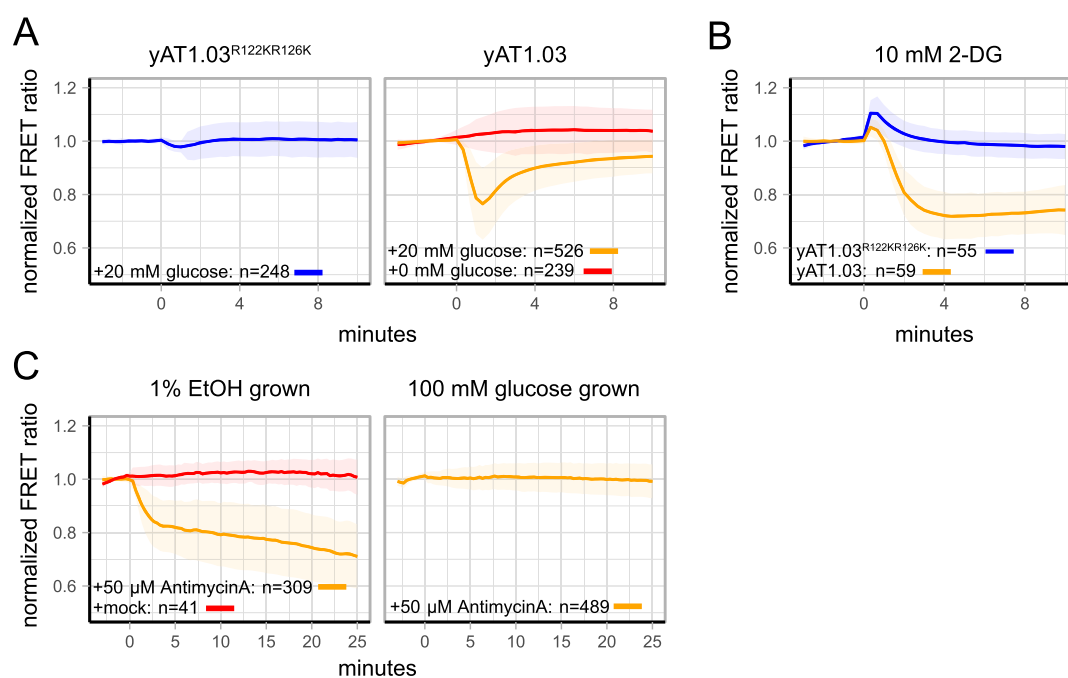


Figure 3. In vivo experiments show reliable yAT1.03 output. (A) W303-1A WT cells expressing yAT1.03 or yAT1.03^{R122KR126K} (depicted above each graph) were grown on 1% EtOH. At $t = 0$ min, glucose or the same medium without glucose was added and the FRET responses were measured. (B) W303-1A WT cells expressing yAT1.03 or yAT1.03^{R122KR126K} were grown with 1% EtOH and incubated in 10 mM glucose for at least 1 h. Afterward, cells were visualized and 10 mM 2-DG was added at $t = 0$ min. (C) W303-1A WT cells expressing yAT1.03 were grown with 1% EtOH or 100 mM glucose as the substrate (depicted above each graph). Antimycin A or only the solvent (mock) was added to the cells at $t = 0$ min. Lines show mean responses, normalized to the baseline, shaded areas indicate SD, and color indicates either the sensor expressed or the added solution. Percentages are v/v, abbreviations: EtOH, ethanol.

observed when medium without glucose was pulsed. The same glucose perturbation did not elicit a response in the non-responsive sensor yAT1.03^{R122KR126K}. These results imply that the sensor indeed measures ATP and no other effects.

Next, we tested if an extreme perturbation of metabolism affects yAT1.03 readouts (Figure 3B). Cells were incubated for 60–90 min in 10 mM glucose after which the glycolytic inhibitor 2-deoxy-D-glucose (2-DG) was added to the cells. 2-DG is transported and phosphorylated by ATP but not further metabolized and thus acts as an ATP drain.^{34,35} FRET responses showed a rapid decrease of FRET, which confirms that the sensor faithfully reports depletion of the ATP pool caused by 2-DG. In contrast, the nonresponsive sensor yAT1.03^{R122KR126K} showed only a minor response, indicating that the yAT1.03 sensor performs robustly in response to extreme metabolic perturbations. This was also confirmed by pulsing 5 mM of glucose to cells lacking *tps1*, which end up in a severe metabolic imbalanced state, with reported low ATP levels and growth arrest (Figure S4).^{17,36} Lastly, we tested whether we could distinguish that ATP is generated by respirative or fermentative metabolism (Figure 3C). Cells were grown with either 1% ethanol as the substrate (ATP generation entirely dependent on respiration) or 100 mM glucose as the substrate (ATP generation largely through fermentation). Subsequently, 50 μ M of antimycin A was added to block respiration through inhibition of the mitochondrial electron transport chain complex III. As anticipated, addition of antimycin A only depleted ATP levels, when cells were growing on ethanol as a substrate. In conclusion, these results demonstrate that yAT1.03 can be used for robust measurements of ATP dynamics in vivo.

Pregrowth Conditions Largely Determine ATP Responses during Transitions. After establishing yAT1.03 as a

robust ATP sensor, we used it to characterize ATP dynamics in response to different carbon source transitions. Cells were grown on various carbon sources and transitioned to glucose (the preferred carbon source) or galactose (Figure 4A). Cells grown on fructose showed only a small transient ATP response when challenged with 100 mM glucose, and no response with 20 mM glucose. In contrast, glucose addition to galactose-grown cells induced the biggest transient decrease of ATP with a mean decrease of 37% in FRET. Lastly, glucose and galactose addition to ethanol-grown cells both show a response, but the responses are qualitatively very different. Glucose addition results in a transient FRET decrease of 24%. In contrast, galactose addition lacked a transient ATP response but showed a steady decrease to the same level compared to glucose, 10 min after addition. Interestingly, both the decrease and recovery of ATP show a high degree of variability between cells, indicating heterogeneity in the responses of individual cells (Figure 4A,B).

Finally, because we were able to conveniently measure ATP in time in living cells, we looked at how ATP levels change in response to multiple successive glucose additions (Figure 4D). The first addition of only 1 mM of glucose to ethanol-growing cells induced a clear transient ATP decrease, but subsequent additions showed only slight responses for most cells. Still, we found heterogeneity again in the responses of individual cells, as can be seen from single-cell traces in Figures 4 and S6.

In summary, we show that ATP dynamics are dependent on the pre-growth condition and show large variations among individual cells. Moreover, for most cells, 1 mM of glucose is sufficient to diminish subsequent ATP responses to further sudden increases in glucose.

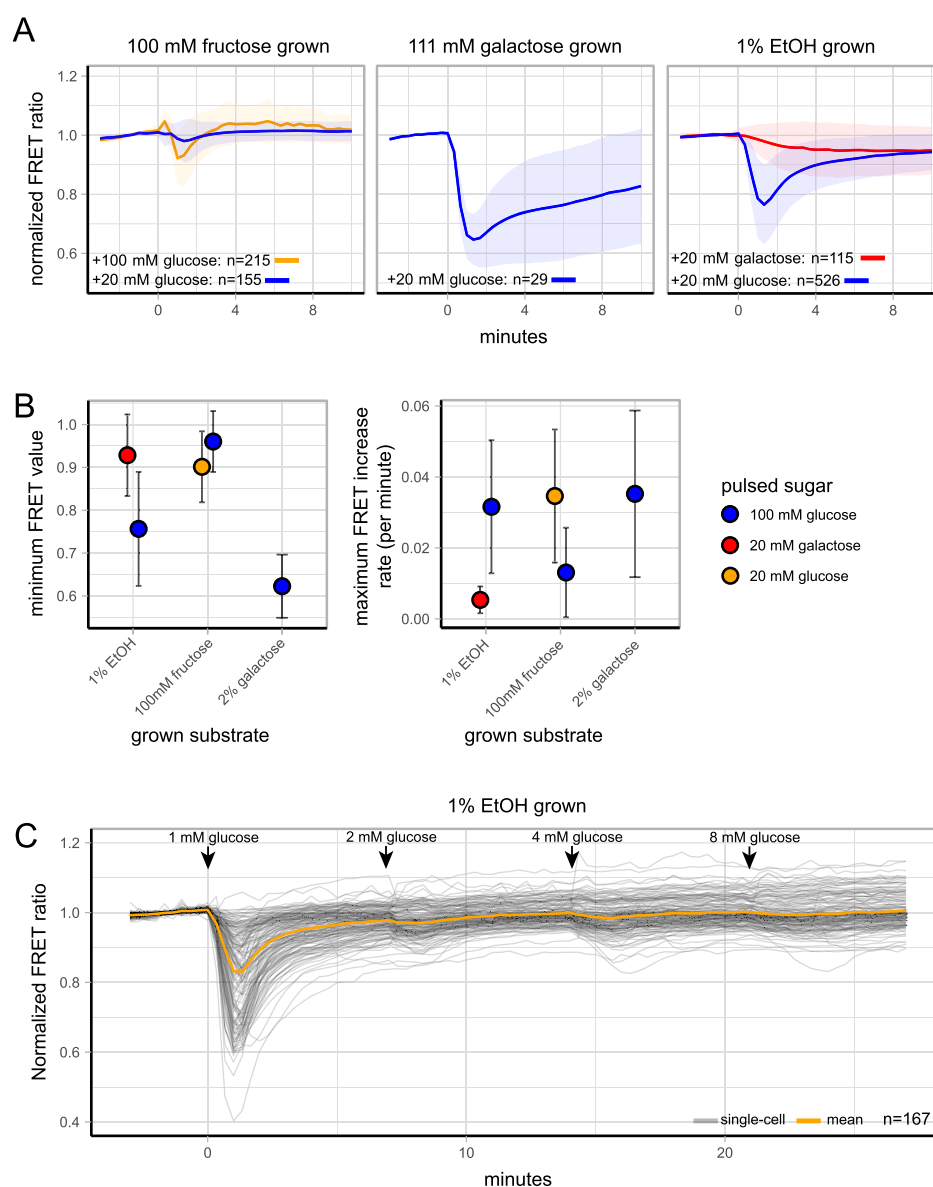


Figure 4. ATP dynamics during various carbon transitions. (A) ATP dynamics of W303-1A cells expressing γ AT1.03 grown on either 1% EtOH, 100 mM fructose, or 111 mM galactose and pulsed with either 20 mM glucose, 100 mM glucose, or 100 mM galactose. Lines show mean FRET ratios, normalized to the baseline, and shade areas indicate SD. (B) Minimum FRET value (i.e., maximum decrease of ATP levels) and ATP recovery speed (depicted by maximum FRET increase per minute) of each transition. Points indicate mean value and error bars indicate SD. (C) ATP dynamics of W303-1A cells expressing γ AT1.03 grown on 1% EtOH and pulsed successively with increasing amounts of glucose. Arrows indicate time points of glucose addition. Orange line show mean FRET ratio (baseline normalized) and grey lines show single-cell traces.

■ ATP DYNAMICS DURING GLYCOLYSIS START-UP ARE HETEROGENEOUS BETWEEN CELLS

Because the ATP responses showed high variability, we looked in more detail at single-cell responses during the ethanol to 20 mM glucose transition (Figure 5). Visualization of the single-cell trajectories and their distributions clearly showed large heterogeneity during the response (Figure 5A,B and Movie S1). We used a hierarchical clustering approach (using Euclidean clustering) to see if dynamic traces can be grouped into distinct response classes (Figure 5C). Next, we determined the optimal cluster amounts (3) using the silhouette method (Figure S5). We identified three types of responses and determined various characteristics for each, such as the absolute baseline FRET ratio (the non-normalized FRET ratio before sugar addition), change in the normalized FRET values at the

end of the timecourse compared to the baseline (Δ FRET), the maximal FRET decrease—(ATP depletion rate) and the increase rate (ATP recovery rate), the minimum FRET value (lowest amount of ATP obtained after the transition), and the time to reach this minimum FRET value (Figure 5D). No difference in the non-normalized baseline FRET values could be found between the clusters, indicating that the starting ATP alone does not determine the ATP dynamics after a transition to glucose. The first cluster contained approximately 61% of all responses and showed a small transient decrease in ATP followed by rapid recovery to preperturbation levels after approximately 8 min. The second cluster contained 36% of the cells and showed a large transient decrease in ATP, followed by fast, but not yet full, recovery after 12 min. A third, smaller cluster contained 3% of all cells and was characterized by rapid ATP depletion, similar to perturbations with either 2-DG or

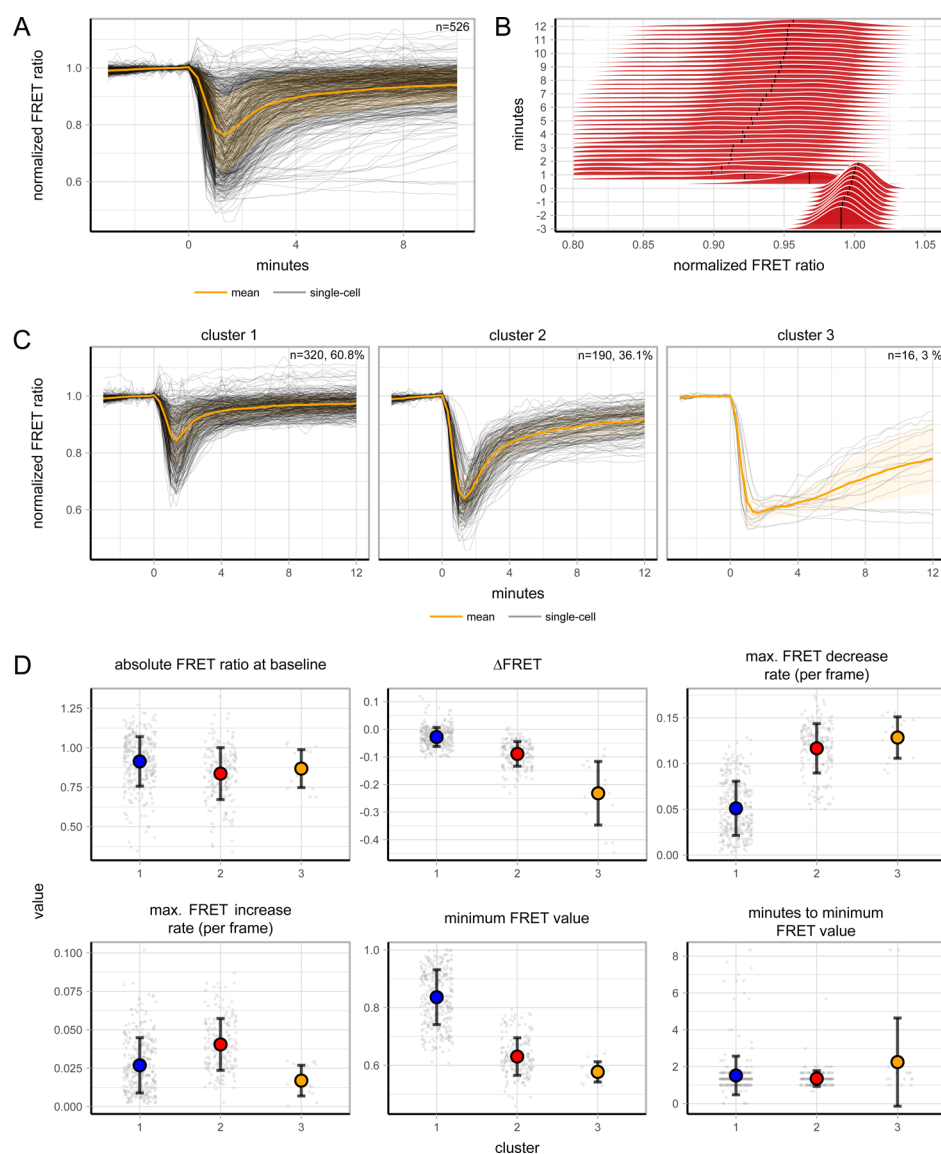


Figure 5. Heterogeneity of cells transitioned from 1% EtOH to 20 mM glucose. (A) ATP dynamics of W303-1A cells expressing γ A1.03 grown on 1% EtOH and pulsed with 20 mM glucose. Orange line shows mean FRET ratio, normalized to the baseline, shades indicate SD, and gray lines show single-cell traces. (B) Normalized frequency distributions of the same transition depicted by graph A. (C) Hierarchical clustering of the single-cell trajectories obtained from graph A showed three distinct subpopulations. Orange lines show normalized mean FRET ratios, shades indicate SD, and gray lines show single-cell traces. (D) Various ATP dynamic parameters per cluster. Absolute FRET ratio at the baseline depicts the mean FRET value (not normalized) of the first 10 frames (before glucose addition); Δ FRET is calculated as the difference of the mean FRET value of the last five frames compared to the baseline. Dots indicate single-cell values, points indicate mean values for each cluster, and error bars indicate SD.

antimycin A (Figure 2), with very slow recovery (or even absent for some cells in this cluster). The absence of ATP recovery in some cells is indicative of an imbalanced metabolic state that cells can get trapped in during these transitions.¹⁷ Such heterogeneous ATP responses were also found when cells were pulsed successively with increasing amounts of glucose (Figure S6). Here, some cells only showed an ATP response after the first glucose pulse and some cells show a response after each addition, while yet others show no responses to any of the perturbations. In contrast to dynamic conditions, steady-state ATP levels of glucose-grown cells showed no clear subpopulations (Figure S8). In summary, we show that glycolytic start-up is highly heterogeneous, ranging in the one extreme from cells that show small or no transient changes in ATP to cells that end up in an imbalanced state with no or little recovery of ATP after a glucose pulse (on short time-scale).

DISCUSSION

Previous work showed that nutrient transitions can result in phenotypic subpopulations and suggested that these subpopulations are a consequence of nongenetic metabolic difference between individual cells.¹⁷ We therefore require tools to study metabolic dynamics at the single-cell level. To gain insights into the dynamics of ATP in single yeast cells, we adapted the AT1.03 sensor to make it more suitable for readouts under dynamic conditions. Specifically, metabolic dynamics in yeast are often characterized by pH changes,^{17,27} and the AT1.03 sensor is sensitive in the physiological pH-range of *S. cerevisiae*.²³ Also, ATP and pH homeostasis are intimately coupled, and this presents an obvious challenge: simultaneous changes in ATP and pH will significantly confound the sensor signal and its interpretation. Furthermore, we found that the original sensor

showed unpredictable baseline drifts (Figure S1), which we believe is caused by photochromicity; this is also affected by pH changes because the mechanisms of photochromism involves (de)protonation of the chromophore.^{37–39} Because photochromic behavior is difficult to be prevented and it hampers characterization of pH effects, we could not reliably characterize the pH sensitivity of the original AT1.03 sensor and compare it directly with yAT1.03. Our modified sensor shows pH stability without photochromic behaviors, in the required physiological range (pH 6.25–7.25) and has a k_d of 3.2 mM, which is optimal, given intracellular ATP concentrations in yeast between 1 and 4 mM.^{14–17,40–43} Our control experiments show that the sensor can be used to reliably measure ATP levels, even for rather extreme metabolic perturbations. First, treatment of fermenting cells with the glycolytic inhibitor 2-DG showed clear ATP drainage. Second, inhibition of the electron transport chain only affects ATP levels in cells growing on ethanol (respiring) and not on glucose (fermenting). In addition, behavior of the non-responsive yAT1.03^{R122KR126K} demonstrated specificity toward ATP.

We characterized ATP dynamics in response to various sudden carbon source transitions as a readout for glycolytic activation. We found that ATP response depended significantly on the combination of pregrowth conditions and pulsed carbon source. For example, galactose-grown cells have a bigger ATP depletion compared to ethanol-grown cells, indicating a large imbalance between ATP consumption and production during start-up of glycolysis (Figure 3). This suggests that cells grown on galactose may have a higher glucose-phosphorylation capacity in the upper part of glycolysis compared to ethanol, which is in line with the fact that galactose is a glycolytic substrate and ethanol is a gluconeogenic one. Indeed, previous reports state that galactose-grown cells have a higher expression of the hexokinases and glucose transport capacity.^{15,44–46} In addition, we show that galactose addition to ethanol-grown cells does not cause a rapid transient decrease in ATP but rather a gradual reduction in ATP levels toward a new steady-state. These differences indicate that galactose does not cause the same transient imbalance in ATP consumption and production that glucose does when cells are precultured on ethanol. Although the first step in galactose metabolism also involves substrate phosphorylation, and therefore ATP consumption, this activity will initially be low as the galactose metabolizing Leloir pathway is only fully induced in the presence of galactose. We also measured ATP dynamics in fructose-grown cells subjected to sudden glucose additions. The small or absent response to glucose indicates that glycolysis is hardly perturbed. This makes sense, as based on growth rates, the glycolytic flux is similar for these sugars (0.37 and 0.35 h⁻¹ for glucose and fructose, respectively, Figure S9). These results combined indicate that the transient ATP decrease is caused by an imbalance between upper (ATP consuming) and lower (ATP producing) parts during the start-up of glycolysis. The timing at which cells experience their minimal ATP levels (minutes of maximal dip) is independent of the extent of ATP decrease (Figures 4A and S7). This suggests that a larger initial ATP depletion is not caused by a longer duration of the upper- and lower-glycolytic imbalance but by the magnitude of the imbalance.

Last, we pulsed cells sequentially with increasing amounts of glucose (Figure 4C). Most cells display a transient decrease of ATP only in response to the first addition of 1 mM glucose. After that, the majority of the cells display no (or diminished) ATP

response to successive glucose additions. Ethanol-grown cells express HXT6 and HXT7 with a K_m around 1 mM.⁴⁵ Apparently, the addition of extra glucose to these cells does not cause a new imbalance between the upper and lower glycolysis.

Our clustering analysis of the ethanol to 20 mM glucose transition (Figure 5) showed that a small fraction of approximately 3% of cells showed this phenotype. An earlier study showed that sudden transitions to glucose cause small populations of cells to end up in a low pH state, a state inferred to indicate an upper- and lower glycolytic imbalance.¹⁷ Our ATP measurements support this inference, showing that indeed a small subpopulation of cells have trouble balancing ATP consumption and production during glycolytic start-up. Previously, it was shown that small variations in metabolic parameters, including enzyme expression levels and metabolite concentrations, determine how a cell will respond to sudden glucose addition. Our data suggest that differences in glycolytic start-up dynamics cannot be explained solely by initial ATP levels (Figure S5).

In conclusion, we provide the yAT1.03 sensor, which shows more robust ATP measurements in yeast cells compared to the original AT1.03 sensor and specifically under dynamic conditions. With this sensor, we could show that ATP dynamics during glycolytic start-up depends on pregrowth conditions and that isogenic cells show highly heterogeneous responses during transitions to glucose. We believe that the yAT1.03 sensor will be a useful addition to the current arsenal of tools to investigate ATP physiology.

■ ASSOCIATED CONTENT

Supporting Information

The Supporting Information is available free of charge at <https://pubs.acs.org/doi/10.1021/acssensors.9b02475>.

Baseline drift of the original AT1.03, ATP levels in the cell-free extract in time, growth of W303-1A cells expressing yAT1.03 or the empty vector pDRF1-GW, response of yAT1.03 and yAT1.03^{R122KR126K} in W303-1A *tps1Δ* cells to a glucose pulse, determination of the optimal number of clusters, single-cell FRET trajectories of cells exposed to multiple glucose pulses, correlation between the maximum decrease of ATP per cell and the timing this dip, steady-state ATP levels of W303-1A cells grown on various substrates, and growth of W303-1A on 10 mM glucose or fructose (PDF)

Ratiometric movie of glucose to ethanol transition of W303-1A WT expressing yAT1.03 (AVI)

■ AUTHOR INFORMATION

Corresponding Author

Bas Teusink — Systems Biology Lab/AIMMS, Vrije Universiteit Amsterdam 1081 HV Amsterdam, The Netherlands; Email: b.teusink@vu.nl

Authors

Dennis Botman — Systems Biology Lab/AIMMS, Vrije Universiteit Amsterdam 1081 HV Amsterdam, The Netherlands; orcid.org/0000-0002-4679-3013

Johan H. van Heerden — Systems Biology Lab/AIMMS, Vrije Universiteit Amsterdam 1081 HV Amsterdam, The Netherlands

Complete contact information is available at:

<https://pubs.acs.org/10.1021/acssensors.9b02475>

Notes

The authors declare no competing financial interest. Plasmids and sequences are available at Addgene (https://www.addgene.org/Bas_Teusink/).

ACKNOWLEDGMENTS

We greatly thank Joachim Goedhart (Molecular Cytology, University of Amsterdam) and Daan de Groot for fruitful discussions.

REFERENCES

- (1) Flamholz, A.; Noor, E.; Bar-Even, A.; Liebermeister, W.; Milo, R. Glycolytic Strategy as a Tradeoff between Energy Yield and Protein Cost. *Proc. Natl. Acad. Sci. U.S.A.* **2013**, *110*, 10039–10044.
- (2) Romano, A. H.; Conway, T. Evolution of Carbohydrate Metabolic Pathways. *Res. Microbiol.* **1996**, *147*, 448–455.
- (3) Delvigne, F.; Zune, Q.; Lara, A. R.; Al-Soud, W.; Sørensen, S. J. Metabolic Variability in Bioprocessing: Implications of Microbial Phenotypic Heterogeneity. *Trends Biotechnol.* **2014**, *32*, 608–616.
- (4) Altschuler, S. J.; Wu, L. F. Cellular Heterogeneity: Do Differences Make a Difference? *Cell* **2010**, *141*, 559–563.
- (5) Xiao, Y.; Bowen, C. H.; Liu, D.; Zhang, F. Exploiting Nongenetic Cell-to-Cell Variation for Enhanced Biosynthesis. *Nat. Chem. Biol.* **2016**, *12*, 339–344.
- (6) Takhaviev, V.; Heinemann, M. Metabolic Heterogeneity in Clonal Microbial Populations. *Curr. Opin. Microbiol.* **2018**, *45*, 30–38.
- (7) DeBerardinis, R. J.; Lum, J. J.; Hatzivassiliou, G.; Thompson, C. B. The Biology of Cancer: Metabolic Reprogramming Fuels Cell Growth and Proliferation. *Cell Metab.* **2008**, *7*, 11–20.
- (8) Chen, Z.; Liu, M.; Li, L.; Chen, L. Involvement of the Warburg Effect in Non-Tumor Diseases Processes. *J. Cell. Physiol.* **2018**, *233*, 2839–2849.
- (9) Efeyan, A.; Comb, W. C.; Sabatini, D. M. Nutrient-Sensing Mechanisms and Pathways. *Nature* **2015**, *517*, 302–310.
- (10) van Heerden, J. H.; Bruggeman, F. J.; Teusink, B. Multi-Tasking of Biosynthetic and Energetic Functions of Glycolysis Explained by Supply and Demand Logic. *BioEssays* **2015**, *37*, 34–45.
- (11) Larsson, C.; Pålman, I.-I.; Gustafsson, L. The importance of ATP as a regulator of glycolytic flux in *Saccharomyces cerevisiae*. *Yeast* **2000**, *16*, 797–809.
- (12) van den Brink, J.; Canelas, A. B.; van Gulik, W. M.; Pronk, J. T.; Heijnen, J. J.; de Winde, J. H.; Daran-Lapujade, P. Dynamics of Glycolytic Regulation during Adaptation of *Saccharomyces Cerevisiae* to Fermentative Metabolism. *Appl. Environ. Microbiol.* **2008**, *74*, 5710–5723.
- (13) Bermejo, C.; Haerizadeh, F.; Takanaga, H.; Chermak, D.; Frommer, W. B. Dynamic Analysis of Cytosolic Glucose and ATP Levels in Yeast Using Optical Sensors. *Biochem. J.* **2010**, *432*, 399–406.
- (14) Walther, T.; Novo, M.; Rössger, K.; Létisse, F.; Loret, M.-O.; Portais, J.-C.; François, J.-M. Control of ATP Homeostasis during the Respiratory-Fermentative Transition in Yeast. *Mol. Syst. Biol.* **2010**, *6*, 344.
- (15) Rolland, F.; Wanke, V.; Cauwenberg, L.; Ma, P.; Boles, E.; Vanoni, M.; Winderickx, J.; Thevelein, J. M.; Winderickx, J. The role of hexose transport and phosphorylation in cAMP signalling in the yeast. *FEMS Yeast Res.* **2001**, *1*, 33–45.
- (16) Hohmann, S.; Bell, W.; Neves, M. J.; Valckx, D.; Thevelein, J. M. Evidence for trehalose-6-phosphate-dependent and -independent mechanisms in the control of sugar influx into yeast glycolysis. *Mol. Microbiol.* **1996**, *20*, 981–991.
- (17) van Heerden, J. H.; Wortel, M. T.; Bruggeman, F. J.; Heijnen, J. J.; Bollen, Y. J. M.; Planque, R.; Hulshof, J.; O'Toole, T. G.; Wahl, S. A.; Teusink, B. Lost in Transition: Start-up of Glycolysis Yields Subpopulations of Nongrowing Cells. *Science* **2014**, *343*, 1245–114.
- (18) Teusink, B.; Walsh, M. C.; van Dam, K.; Westerhoff, H. V. The Danger of Metabolic Pathways with Turbo Design. *Trends Biochem. Sci.* **1998**, *23*, 162–169.
- (19) Martinez-Outschoorn, U. E.; Peiris-Pagés, M.; Pestell, R. G.; Sotgia, F.; Lisanti, M. P. Cancer Metabolism: A Therapeutic Perspective. *Nat. Rev. Clin. Oncol.* **2017**, *14*, 11–31.
- (20) Swanton, C. Intratumor Heterogeneity: Evolution through Space and Time. *Cancer Res.* **2012**, *72*, 4875–4882.
- (21) Pribluda, A.; de la Cruz, C. C.; Jackson, E. L. Intratumoral Heterogeneity: From Diversity Comes Resistance. *Clin. Cancer Res.* **2015**, *21*, 2916–2923.
- (22) Inde, Z.; Dixon, S. J. The Impact of Non-Genetic Heterogeneity on Cancer Cell Death. *Crit. Rev. Biochem. Mol. Biol.* **2018**, *53*, 99–114.
- (23) Imamura, H.; Huynh Nhat, K. P.; Togawa, H.; Saito, K.; Iino, R.; Kato-Yamada, Y.; Nagai, T.; Noji, H. Visualization of ATP Levels inside Single Living Cells with Fluorescence Resonance Energy Transfer-Based Genetically Encoded Indicators. *Proc. Natl. Acad. Sci. U.S.A.* **2009**, *106*, 15651–15656.
- (24) Takaine, M.; Ueno, M.; Kitamura, K.; Imamura, H.; Yoshida, S. Reliable Imaging of ATP in Living Budding and Fission Yeast. *J. Cell Sci.* **2019**, *132*, jcs230649.
- (25) Botman, D.; de Groot, D. H.; Schmidt, P.; Goedhart, J.; Teusink, B. In Vivo Characterisation of Fluorescent Proteins in Budding Yeast. *Sci. Rep.* **2019**, *9*, 2234.
- (26) Orij, R.; Urbanus, M. L.; Vizeacoumar, F. J.; Giaever, G.; Boone, C.; Nislow, C.; Brul, S.; Smits, G. J. Genome-wide analysis of intracellular pH reveals quantitative control of cell division rate by pHc in *Saccharomyces cerevisiae*. *Genome Biol.* **2012**, *13*, R80.
- (27) Orij, R.; Postmus, J.; Ter Beek, A.; Brul, S.; Smits, G. J. In vivo measurement of cytosolic and mitochondrial pH using a pH-sensitive GFP derivative in *Saccharomyces cerevisiae* reveals a relation between intracellular pH and growth. *Microbiology* **2009**, *155*, 268–278.
- (28) Thevelein, J. M.; Beullens, M.; Honshoven, F.; Hoebeek, G.; Detremere, K.; GRIEWEL, B.; Den Hollander, J. A.; Jans, A. W. H. Regulation of the cAMP Level in the Yeast *Saccharomyces Cerevisiae*: The Glucose-Induced cAMP Signal Is Not Mediated by a Transient Drop in the Intracellular PH. *Microbiology* **1987**, *133*, 2197–2205.
- (29) Kresnowati, M. T. A. P.; Suarez-Mendez, C. M.; van Winden, W. A.; van Gulik, W. M.; Heijnen, J. J. Quantitative Physiological Study of the Fast Dynamics in the Intracellular PH of *Saccharomyces Cerevisiae* in Response to Glucose and Ethanol Pulses. *Metab. Eng.* **2008**, *10*, 39–54.
- (30) Kresnowati, M. T. A. P.; Suarez-Mendez, C. M.; van Winden, W. A.; van Gulik, W. M.; Heijnen, J. J. Quantitative Physiological Study of the Fast Dynamics in the Intracellular PH of *Saccharomyces Cerevisiae* in Response to Glucose and Ethanol Pulses. *Metab. Eng.* **2008**, *10*, 39–54.
- (31) Gietz, R. D.; Schiestl, R. H. Quick and Easy Yeast Transformation Using the LiAc/SS Carrier DNA/PEG Method. *Nat. Protoc.* **2007**, *2*, 35–37.
- (32) Hansen, A. S.; Hao, N.; O'Shea, E. K. High-Throughput Microfluidics to Control and Measure Signaling Dynamics in Single Yeast Cells. *Nat. Protoc.* **2015**, *10*, 1181–1197.
- (33) Botman, D.; O'Toole, T.; Goedhart, J.; Bruggeman, F. J.; van Heerden, J. H.; Teusink, B. A FRET Biosensor Enlightens cAMP Signalling in Budding Yeast. *bioRxiv* **2019**, 831354.
- (34) Cramer, F. B.; Woodward, G. E. 2-Desoxy-D-Glucose as an Antagonist of Glucose in Yeast Fermentation. *J. Franklin Inst.* **1952**, *253*, 354–360.
- (35) Wick, A. N.; Drury, D. R.; Nakada, H. I.; Wolfe, J. B. Localization of the Primary Metabolic Block Produced by 2-Deoxyglucose. *J. Biol. Chem.* **1957**, *224*, 963–969.
- (36) Peeters, K.; Van Leemputte, F.; Fischer, B.; Bonini, B. M.; Quezada, H.; Tsytlonok, M.; Haesen, D.; Vanthienen, W.; Bernardes, N.; Gonzalez-Blas, C. B.; et al. Fructose-1,6-Bisphosphate Couples Glycolytic Flux to Activation of Ras. *Nat. Commun.* **2017**, *8*, 992.
- (37) Brakemann, T.; Weber, G.; Andresen, M.; Groenhof, G.; Stiel, A. C.; Trowitzsch, S.; Eggeling, C.; Grubmüller, H.; Hell, S. W.; Wahl, M. C.; et al. Molecular Basis of the Light-Driven Switching of the Photochromic Fluorescent Protein Padron. *J. Biol. Chem.* **2010**, *285*, 14603–14609.

(38) Mizuno, H.; Mal, T. K.; Walchli, M.; Kikuchi, A.; Fukano, T.; Ando, R.; Jeyakanthan, J.; Taka, J.; Shiro, Y.; Ikura, M.; et al. Light-Dependent Regulation of Structural Flexibility in a Photochromic Fluorescent Protein. *Proc. Natl. Acad. Sci. U.S.A.* **2008**, *105*, 9227–9232.

(39) Dean, K. M.; Lubbeck, J. L.; Binder, J. K.; Schwall, L. R.; Jimenez, R.; Palmer, A. E. Analysis of Red-Fluorescent Proteins Provides Insight into Dark-State Conversion and Photodegradation. *Biophys. J.* **2011**, *101*, 961–969.

(40) Albe, K. R.; Butler, M. H.; Wright, B. E. Cellular Concentrations of Enzymes and Their Substrates. *J. Theor. Biol.* **1990**, *143*, 163–195.

(41) Lagunas, R.; Gancedo, C. Role of phosphate in the regulation of the Pasteur effect in *Saccharomyces cerevisiae*. *Eur. J. Biochem.* **1983**, *137*, 479–483.

(42) Bañuelos, M.; Gancedo, C.; Gancedo, J. M. Activation by Phosphate of Yeast Phosphofructokinase. *J. Biol. Chem.* **1977**, *252*, 6394–6398.

(43) Park, J. O.; Rubin, S. A.; Xu, Y.-F.; Amador-Noguez, D.; Fan, J.; Shlomi, T.; Rabinowitz, J. D. Metabolite Concentrations, Fluxes and Free Energies Imply Efficient Enzyme Usage. *Nat. Chem. Biol.* **2016**, *12*, 482–489.

(44) Herrero, P.; Galíndez, J.; Ruiz, N.; Martínez-Campa, C.; Moreno, F. Transcriptional regulation of the *Saccharomyces cerevisiae* HXK1, HXK2 and GLK1 genes. *Yeast* **1995**, *11*, 137–144.

(45) Maier, A.; Völker, B.; Boles, E.; Fuhrmann, G. F. Characterisation of glucose transport in *Saccharomyces cerevisiae* with plasma membrane vesicles (countertransport) and intact cells (initial uptake) with single Hxt1, Hxt2, Hxt3, Hxt4, Hxt6, Hxt7 or Gal2 transporters. *FEMS Yeast Res.* **2002**, *2*, 539–550.

(46) Reifenberger, E.; Boles, E.; Ciriacy, M. Kinetic Characterization of Individual Hexose Transporters of *Saccharomyces Cerevisiae* and Their Relation to the Triggering Mechanisms of Glucose Repression. *Eur. J. Biochem.* **1997**, *245*, 324–333.